Partial Distinguishability in Femtosecond Optical Spontaneous Parametric Down-Conversion

Mete Atatüre,[1] Alexander V. Sergienko,[2] Bradley M. Jost,[2] Bahaa E. A. Saleh,[2] and Malvin C. Teich[1,2]

[1]*Quantum Imaging Laboratory, Department of Physics, Boston University, 8 Saint Mary's Street, Boston, Massachusetts 02215*
[2]*Quantum Imaging Laboratory, Department of Electrical and Computer Engineering, Boston University, 8 Saint Mary's Street, Boston, Massachusetts 02215*

Quantum interference is observed using femtosecond parametric down-conversion in the absence of spectral filtering of the down-converted light. The well-known symmetric dip observed in cw polarization-interferometry experiments becomes less pronounced and substantially asymmetric under such pulsed excitation. We show that this asymmetry arises from the partial distinguishability of contributions from space-time segments within the down-conversion crystal. We develop a theory that achieves agreement with experiment by coherently adding intrasegment contributions while incoherently adding intersegment contributions.

Entangled photon pairs (biphotons) generated via the nonlinear optical process of spontaneous parametric down-conversion (SPDC) [1,2] have enabled us to carry out many valuable quantum-optics experiments, particularly during the past few years. These range from fundamental physics experiments that have shed light on the validity of quantum mechanics [3,4] to useful applications such as the determination of detector absolute quantum efficiency [5]. Entangled photon pairs have recently also found a place in unusual but powerful techniques such as quantum cryptography [6] and quantum teleportation [7,8].

Almost all of these experiments have made use of stationary streams of biphotons generated by illuminating an anisotropic second-order nonlinear crystal with a continuous-wave (cw) laser pump. The unique possibilities offered by such light sources reside in their entanglement property, which is mathematically described in terms of a composite quantum state that cannot be factored into a produce of single-particle states (entangled states thereby have no classical analogs) [9]. A great variety of quantum-interference experiments have been carried out to examine the unusual second- and fourth-order coherence properties [10,11] of partially entangled biphoton beams.

Since ultrafast (sub-ps) pump sources in the ultraviolet and near-ultraviolet have come into their own, it is important to determine the entanglement properties imparted to biphoton beams by very brief pulses of pump light impinging on a nonlinear parametric down-conversion crystal. The reason is simple: entangled photon pairs generated by mode-locked pump lasers emitting femtosecond pulses are expected to be crucial for carrying out important experiments in quantum teleportation [12], entanglement swapping [13], and the production of three-photon entangled [Greenberger-Horne-Zeilinger (GHZ)] states [14]. Several experiments along these lines have already been conducted. Some of these have made use of crystals whose lengths are short relative to the length of the coherent nonlinear interaction region [15]. Others have employed narrow-band interference filters placed immediately

before the detectors [12,13,15,16]. The filters serve to lengthen the coherence time of the photons and thereby to increase the fringe visibility in interference experiments. Although the results of both of these types of experiments can be understood within the constraints of existing theories [15–18], the biphoton state is irreversibly altered by the presence of the filters so that the intrinsic entanglement associated with the original femtosecond biphotons is obfuscated.

The purpose of this Letter is to demonstrate, both experimentally and theoretically, that the entanglement properties of *unfiltered* down-converted biphoton pulses are distinctly different from those generated by a cw pump. They depend strongly on the ratio of the coherent-interaction and crystal lengths. Their properties are readily manifested in fourth-order biphoton polarization-interference experiments (see Fig. 1) using SPDC crystals of different lengths (shorter than, of the order of, and longer than the coherent nonlinear interaction length for the femtosecond pump pulse). As in the cw case symmetric fourth-order interference dips are the order of the day for short crystals; however, distinct and unusual asymmetries emerge in the dips when long crystals are
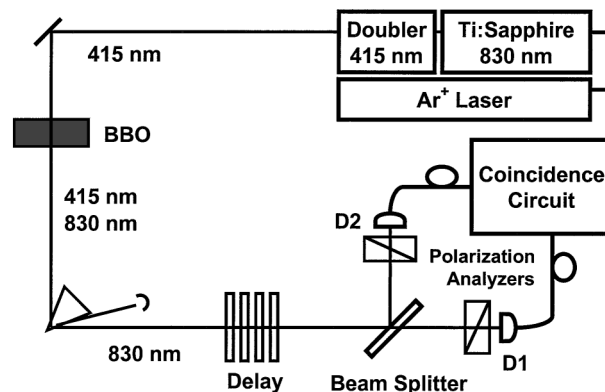
FIG. 1. Schematic of the experimental setup for observation of fourth-order quantum interference using femtosecond SPDC.

used. We develop a new theoretical model for femtosecond biphoton generation via down-conversion that explains these observations: The asymmetries arise from partially distinguishable biphoton contributions associated with different segments within the crystal.

Nonstationary SPDC theory.—For simplicity, we assume collinear (along the z axis) one-dimensional down-conversion. SPDC is assumed to arise through a first-order time-dependent perturbation on the vacuum state, in which the interaction Hamiltonian contributes only when the pump pulse lies within the crystal. When the pump pulse is short, at any given time the signal, idler, and pump beams overlap only over a small subregion of the crystal, within which they contribute coherently to the coincidence probability. The various subregions, however, contribute incoherently with each other. In the cw case, at all times the beams overlap throughout the length of the crystal L, so that the entire interaction process is fully coherent. Previous theoretical models of ultrafast SPDC are based on the assumption of fully coherent contributions over the entire crystal length [15–18], as is the case for cw SPDC. The feature that is unique to our theory is the finiteness of the interaction length imposed by the partial temporal overlap of the pump pulse and the down-converted wave packets within the crystal.

The two-photon state for each down-converted pair thus depends on the particular location of the region from which the pair originates. We use the symbol ξ to denote the location of this interaction volume. The variable ξ is regarded as a uniformly distributed random position in the crystal, which indexes the location of the coherent region from which the photon pair is emitted. The perturbed state is then a function of a localized interaction Hamiltonian around ξ,

$$|\Psi_\xi^{(2)}\rangle \sim |0\rangle - \frac{i}{\hbar} \int_{t_0}^{t} dt' \hat{H}_{\text{int}}(t', \xi) |0\rangle \quad (1)$$

with

$$\hat{H}_{\text{int}}(t', \xi) \sim \chi^{(2)} \int_{-L}^{0} dz \, W(z - \xi) E_p^{(+)}(t', z)$$
$$\times E_s^{(-)}(t', z) E_i^{(-)}(t', z) + \text{H.c.}, \quad (2)$$

where $\chi^{(2)}$ indicates the second-order susceptibility; $E^{(+)}$ and $E^{(-)}$ represent the positive- and negative-frequency portion of the electric-field operator, respectively; and the subscripts p, s, and i represent the pump, signal, and idler waves, respectively. Because of its relatively high intensity, the pump field is treated classically in terms of a propagating transform-limited polychromatic wave packet with a Gaussian-intensity profile $I_p(t, z)$. The function $W(z - \xi)$, which we refer to as the *partial decoherence function,* identifies the degree of distinguishability due to partial overlap in space-time of the three wave packets (pump, signal, and idler) as they propagate through the nonlinear crystal. This function, which is conjectured to be proportional to the area of overlap among the three wave packets, monotonically decreases as its argument increases, since the signal and idler wave packets gradually

separate from the pump as a result of their different group velocities. Numerical calculation of the area of mutual overlap for our Gaussian wave packets shows that the partial decoherence function may be well approximated by a single-sided Gaussian function of width d_{eff}:

$$W(z - \xi) = \exp\left\{-\left(\frac{z - \xi}{d_{\text{eff}}}\right)^2\right\} \text{rect}_{[-L,0]}(z - \xi). \quad (3)$$

The rect function is unity within its range and zero elsewhere.

Equation (2) is therefore delineated by an interaction region of characteristic length d_{eff} surrounding the location ξ. This localized interaction Hamiltonian results in a two-photon wave function that explicitly bears the stamp of where in the crystal the pair is generated. The two-photon probability amplitude

$$A_\xi(t_1, t_2) = \langle 0|\hat{E}_2^{(+)}(z_2, t_2)\hat{E}_1^{(+)}(z_1, t_1)|\Psi_\xi^{(2)}\rangle \quad (4)$$

is therefore not identical for every down-converted pair, because of its dependence on the localization region (around ξ) in the nonlinear crystal where the down-converted pair is generated. Consequently, as illustrated in Fig. 2, two regions within the crystal separated by a distance greater than d_{eff} emit *distinguishable* pairs of down-converted photons. Using Eq. (3), the two-photon probability amplitude may be written in terms of the detection time difference $t = (t_1 - t_2)$ and the mean detection time $T = (\frac{t_1 + t_2}{2})$ in the form

$$A_\xi(T, t) \sim \sqrt{I_p\left(T - \frac{\Lambda}{D} t - \frac{\xi}{v_p}\right)}$$
$$\times W(t) \text{rect}_{[-L,0]}\left(\xi + \frac{t}{D}\right) e^{i(k_p^0 \xi - \omega_p^0 T)}, \quad (5)$$

where k_p^0 and ω_p^0 are the central wave number and circular frequency of the pump, respectively, $D = (\frac{1}{v_i} - \frac{1}{v_s})$ is
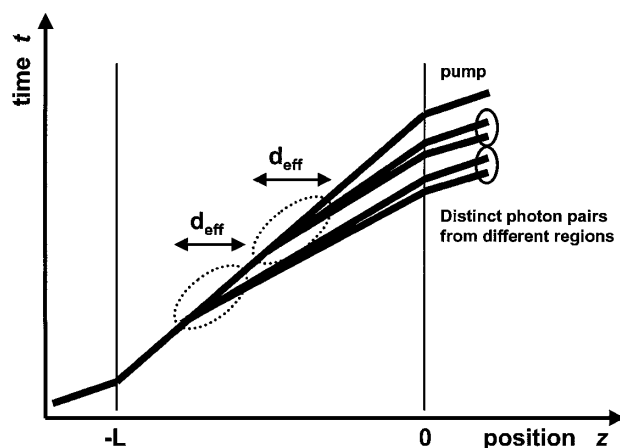
FIG. 2. Space-time diagram illustrating two partially overlapping segments of length d_{eff} within the crystal. Intrasegment contributions (within d_{eff}) are added coherently, whereas intersegment contributions are added incoherently. The vertical thickness of each beam represents its temporal duration. In the cw case, the pump has infinite duration and overlaps all beams at all times.

the group velocity dispersion for the signal and idler waves, and $\Lambda = [\frac{1}{v_p} - \frac{1}{2}(\frac{1}{v_i} + \frac{1}{v_s})]$.

We now use this result to determine the fourth-order coincidence rate in accordance with the usual procedure for quantum-interference experiments. Consider the generation of entangled-photon states by pump pulses of

duration τ_p in a type-II nonlinear crystal of length L followed by a variable length of birefringent material which acts as an optical delay line τ that feeds a polarization interferometer (see Fig. 1). The contribution to the total coincidence rate R for a particular down-converted pair generated in the vicinity of location ξ in the nonlinear crystal can be written as

$$R_\xi(\tau) \sim \frac{1}{2} \int_{-\infty}^{\infty} \int_{-\infty}^{\infty} dT\, dt\, |A_\xi(T,t)|^2 - \frac{1}{2} \mathrm{Re}\left[\int_{-\infty}^{\infty} \int_{-\infty}^{\infty} dT\, dt\, A_\xi(T, t + \tau) A_\xi^*(T, -t + \tau) \right]. \tag{6}$$

Detection over many down-converted photon pairs requires the ensemble averaging over all possible values of ξ within the crystal. This ensemble averaging process yields an integral over the variable ξ, so that the observed overall normalized coincidence rate as a function of optical delay τ in the polarization quantum interferometer becomes

$$R_N(\tau) = \begin{cases} 1 - \dfrac{\int_{-L+d_{\mathrm{eff}}}^{0} d\xi \int_{-\infty}^{\infty} \int_{-\infty}^{\infty} dT\, dt\, \mathrm{Re}[A_\xi(T,t+\tau)A_\xi^*(T,-t+\tau)]}{\int_{-L+d_{\mathrm{eff}}}^{0} d\xi \int_{-\infty}^{\infty} \int_{-\infty}^{\infty} dT\, dt\, |A_\xi(T,t)|^2}, & \text{if } \dfrac{d_{\mathrm{eff}}}{L} \leq 1, \\[3ex] 1 - \dfrac{\int_{-\infty}^{\infty} \int_{-\infty}^{\infty} dT\, dt\, \mathrm{Re}[A_0(T,t+\tau)A_0^*(T,-t+\tau)]}{\int_{-\infty}^{\infty} \int_{-\infty}^{\infty} dT\, dt\, |A_0(T,t)|^2}, & \text{if } \dfrac{d_{\mathrm{eff}}}{L} \gg 1. \end{cases} \tag{7}$$

Equation (7) is our principal theoretical result. If the ratio d_{eff}/L is large, the entire crystal behaves as a single region, contributing coherently to the overall coincidence rate. Just as in the cw case the interference dip is then symmetric, and almost triangular, and exhibits nearly 100% visibility (solid curve in the top graph of Fig. 3). The physical length of the nonlinear crystal can be readily determined from the width of the interference dip. In the opposite limit, when d_{eff}/L is sufficiently small such as is the case for ultrafast down-conversion, decoherence effects become important and the result is a strongly asymmetric interference dip with reduced visibility (solid curve in the bottom graph of Fig. 3). Thus the character of the interference dip is dependent on a combination of the crystal length and the pump-pulse duration. The ratio of the interference-dip width to the nonlinear crystal length does not remain constant, unlike the case for cw-pumped SPDC and all previous theories involving ultrafast pump pulses.

Nonstationary SPDC interference experiment.— We have carried out an experiment using nonlinear type-II-cut beta-barium borate (BBO) crystals of three different lengths without using any spectral filtering of the down-converted light. A schematic of the experimental arrangement is shown in Fig. 1. An Ar^+-ion laser serves as a pump for a mode-locked Ti:sapphire laser whose light, in turn, is doubled in a second-harmonic generator. The result is a train of 80-fs pulses with an 82-MHz repetition rate, a central wavelength of 415 nm, and an average power of about 15 mW. Three separate experiments were performed to produce collinear and degenerate ($\omega_1^0 = \omega_2^0 = \omega_p^0/2$) SPDC, using crystal lengths of 0.5, 1.5, and 3 mm. A circular 2.5-mm-diameter aperture position 7 cm from the nonlinear crystal was used to eliminate noncollinear pairs. The residual pump light was removed from the signal and idler beams by passing all of them through a fused silica dispersion prism and using an iris. The collinear beams were then sent through a delay line comprised of a crystalline quartz element (fast axis orthogonal to the fast axis of the BBO crystal)

whose thickness could be varied to alter the delay between the photons of a down-converted pair. The photon pairs were then sent to a nonpolarizing beam splitter. Each arm of the polarization intensity interferometer following this beam splitter contained a Glan-Thompson polarization analyzer at 45°, a convex lens to focus the incoming beam, and an actively quenched Peltier-cooled single-photon-counting avalanche photodiode detector (denoted D in Fig. 1) that was placed approximately 1 m away from the beam splitter. No spectral filtering was used in the selection of the signal and idler photons for detection. The counts from the detectors were sent to a coincidence counting circuit with a 3-ns coincidence-time window. The integration time was 100 seconds, yielding experimental errors determined principally by the statistics of the number of coincidences. Background was not subtracted from the data.

Discussion.— The experimentally observed normalized coincidence rates (open circles) are displayed in Fig. 3 as a function of the relative optical delay (determined by the thickness of the quartz element). Results are presented for BBO crystals of three lengths: 0.5 mm (top), 1.5 mm (middle), and 3 mm (bottom). The theoretically expected normalized coincidence rates, presented as the solid curves in Fig. 3, were obtained using the known physical constants for BBO along with Eqs. (3), (5), and (7). The value of d_{eff}, which turns out to be ~ 1.4 mm, was determined by evaluating the $1/e$ width of the overlap area among the three Gaussian wave packets. The agreement between theory and experiment, which involved no free parameters, shows that decoherence provides a proper characterization of femtosecond SPDC. The 0.5-mm crystal is thinner than the length of coherent interaction in the BBO crystal, so that the width of the symmetric dip pattern is determined principally by the physical length of the crystal. On the other hand, the 3.0-mm crystal exhibits a highly asymmetric pattern and the dip width reveals no information about the crystal length.
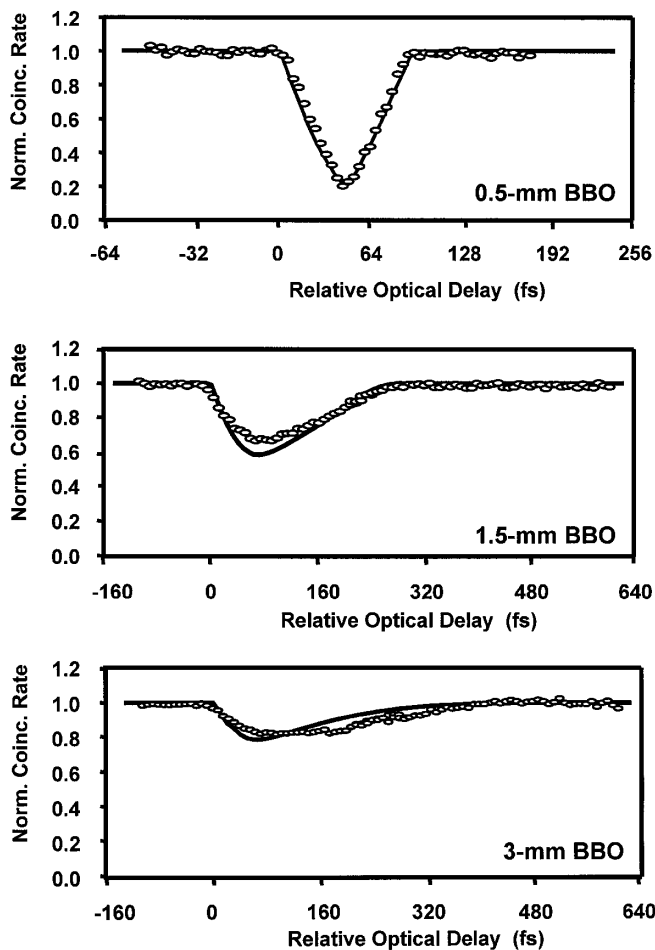
FIG. 3. Experimental (open circles) and theoretical (solid curves) results for the normalized coincidence rate for BBO crystals of three different lengths (top: 0.5 mm; center: 1.5 mm; bottom: 3.0 mm) as a function of the relative optical path delay τ. As the crystal length increases, the fringe visibility diminishes substantially and a dramatic asymmetry emerges.

The intermediate case involving the 1.5-mm crystal lies in the transition region between the two distinct limits of Eq. (7), since the ratio d_{eff}/L has a value close to 1 in our experiment. However, the close resemblance of the experimental results and the theoretical prediction shows that the model we have developed for nonstationary SPDC with ultrafast pump pulses has broad validity for all values of the ratio d_{eff}/L. We expect similar effects in the interference patterns for type-I SPDC with ultrashort pump pulses.

The inclusion of second-order dispersion associated with the nonlinear crystal and birefringent delay line [19] will slightly modify the fit between theory and experiment. These modifications will not, however, significantly alter the asymmetry of the interference pattern for typical values of second-order dispersion parameters.

In summary, despite the coherent nature of the pump pulse, the process of quantum interference is nevertheless not entirely coherent. This is because it results from an ensemble average of contributions from different independent interaction regions within the down-conversion crys-

tal, each of which has its own Hamiltonian. In the cw case, that region is the entire width of the crystal which is the same for every realization of the ensemble. The nature of the decoherence operative in this process is in probability space, which is distinct from the decoherence resulting from dephasing associated with propagation.

[1] D. C. Burnham and D. L. Weinberg, Phys. Rev. Lett. **25**, 84 (1970).

[2] J. Peřina, Z. Hradil, and B. Jurčo, *Quantum Optics and Fundamentals of Physics* (Kluwer, Boston, 1994).

[3] J. S. Bell, Physics (Long Island City, N.Y.) **1**, 195 (1964).

[4] C. K. Hong, Z. Y. Ou, and L. Mandel, Phys. Rev. Lett. **59**, 1903 (1987); Y. H. Shih and C. O. Alley, Phys. Rev. Lett. **61**, 2921 (1988).

[5] D. N. Klyshko, Sov. J. Quantum Electron. **7**, 591 (1977); A. Migdall, R. Datla, A. V. Sergienko, J. S. Orszak, and Y. H. Shih, Appl. Opt. **37**, 3455 (1998).

[6] A. K. Ekert, Phys. Rev. Lett. **67**, 661 (1991); J. G. Rarity and P. R. Tapster, Phys. Rev. A **45**, 2052 (1992).

[7] C. H. Bennett, G. Brassard, C. Crepeau, R. Jozsa, A. Peres, and W. Wootters, Phys. Rev. Lett. **70**, 1895 (1993).

[8] D. Boschi, S. Branca, F. De Martini, L. Hardy, and S. Popescu, Phys. Rev. Lett. **80**, 1121 (1998).

[9] E. Schrödinger, Naturwissenschaften **23**, 807 (1935); **23**, 823 (1935); **23**, 844 (1935) [translation in *Quantum Theory and Measurement,* edited by J. A. Wheeler and W. H. Zurek (Princeton University Press, Princeton, NJ, 1983)].

[10] B. E. A. Saleh, A. Joobeur, and M. C. Teich, Phys. Rev. A **57**, 3991 (1998).

[11] A. V. Sergienko, Y. H. Shih, and M. H. Rubin, J. Opt. Soc. Am. B **12**, 859 (1995).

[12] D. Bouwmeester, J.-W. Pan, K. Mattle, M. Eibl, H. Weinfurter, and A. Zeilinger, Nature (London) **390**, 575 (1997).

[13] J.-W. Pan, D. Bouwmeester, H. Weinfurter, and A. Zeilinger, Phys. Rev. Lett. **80**, 3891 (1998).

[14] D. M. Greenberger, M. Horne, and A. Zeilinger, in *Bell's Theorem, Quantum Theory, and Conceptions of the Universe,* edited by M. Kafatos (Kluwer, Dordrecht, 1989); D. M. Greenberger, M. A. Horne, A. Shimony, and A. Zeilinger, Am. J. Phys. **58**, 1131 (1990); A. Zeilinger, M. A. Horne, H. Weinfurter, and M. Zukowski, Phys. Rev. Lett. **78**, 3031 (1997).

[15] W. P. Grice, R. Erdmann, I. A. Walmsley, and D. Branning, Phys. Rev. A **57**, R2289 (1998).

[16] G. Di Giuseppe, L. Haiberger, F. De Martini, and A. V. Sergienko, Phys. Rev. A **56**, R21 (1997).

[17] W. P. Grice and I. A. Walmsley, Phys. Rev. A **56**, 1627 (1997).

[18] T. E. Keller and M. H. Rubin, Phys. Rev. A **56**, 1534 (1997).

[19] J. Peřina, Jr., A. V. Sergienko, B. M. Jost, B. E. A. Saleh, and M. C. Teich, Phys. Rev. A **59**, 2359 (1999).